Received: 28 October 2021 | Accepted: 20 January 2022

DOI: 10.1111/gcbb.12939

GCB-BIOENERGY BIOPRODUCTS FOR A SUSTAINABLE BIOECONOMY Open Access

WILEY

RESEARCH ARTICLE

Identification of early abandonment in cropland through radar-based coherence data and application of a Random-Forest model

Wouter Meijninger[1] | **Berien Elbersen**[1] | **Michiel van Eupen**[1] | **Stephan Mantel**[2] | **Pilar Ciria**[3] | **Andrea Parenti**[4] | **Marina Sanz Gallego**[3] | **Paloma Perez Ortiz**[3] | **Marco Acciai**[4] | **Andrea Monti**[4]

[1]Wageningen University & Research, Wageningen, The Netherlands

[2]ISRIC, Wageningen, The Netherlands

[3]CIEMAT, Madrid, Spain

[4]Bologna University, Bologna, Italy

Correspondence
Berien Elbersen, Wageningen University & Research, Wageningen, The Netherlands.
Email: berien.elbersen@wur.nl

Funding information
European Union's Horizon 2020 Research and Innovation Program, Grant/Award Number: 727698

Abstract

In the context of increased pressures on land for food and non-food production, it is relevant to understand better, which land resources have become unused and abandoned and where these lands are. Data on where these lands are and what their extend is are not collected in regular statistics. In this paper, we present an approach to detect signs of abandonment in cropping land using radar coherence data. The methodology was tested in the Spanish regions of Albacete and Soria where agricultural land abandonment is a common process. The results show that land abandonment detection using radar coherence data works well for the region of Albacete in arable lands. The radar-based analysis is a relatively simple method to detect land abandonment in an early to longer term state and can therefore be applied once developed and tested further in other regions to larger areas of the EU where land abandonment is serious and needs monitoring and policy response. The applicability of the method to Soria and Emilia Romagna (Italy) regions shows that there are still challenges to overcome to make the method more widely applicable for detecting land abandonment in other environmental zones of Europe. Lack of reliable training and validation data, like Land Parcel Identification Systems data, in regions is one of the challenges in this respect.

KEYWORDS

abandoned lands, radar coherence, satellite remote sensing, unused lands

1 | INTRODUCTION

The demand for biomass for nonfood uses is expected to increase because ambitions to develop the bioeconomy further as an instrument to decarbonize the fossil-intensive sectors. The potential of sustainable biomass is limited (Allen et al., 2014; Thrän et al., 2010) and indirect land use effects need to be avoided (Daioglou et al., 2020;

Wouter Meijninger and Berien Elbersen contributed equally to this work.

EC Directorate-General for Research and Innovation, 2018). Residual biomass, for example, primary residues from agriculture and forests, organic wastes are seen as the more sustainable biomass feedstocks, particularly because there are no or limited direct (dLUC) and indirect land use change (iLUC) effects (Daioglou et al., 2020; EC Directorate-General for Research and Innovation, 2018; Overmars et al., 2015; Valin et al., 2015). However, residues and waste sources alone will not be enough to satisfy the expected future biomass demands (e.g., OECD, 2018; Pelkmans et al., 2016; Plevin et al., 2015; Valin et al., 2015). Additional sourcing from dedicated cropping of biomass is needed to satisfy rising demands. These new demands may have effects on land use, biodiversity, and other ecosystem services and compete with food production (Daioglou et al., 2020; Edwards et al., 2010; ETC/SIA, 2013; Fargione et al., 2010; Searchinger et al., 2008). One of the options to avoid iLUC effects is through the use of unused and abandoned lands which have both already been envisaged as land resources for the delivery of low iLUC biomass for biofuel production in the EU Recast Renewable Energy Directive RED II (EC Directorate-General for Research and Innovation, 2018). This study will focus on the detection of abandoned lands which are defined as in the RED II as: *unused land which was used in the past for the cultivation of food and feed crops, but where this cultivation ended, for at least five consecutive years, due to biophysical or socio-economic constraints*.

The key assumption in all studies on abandoned lands for bioenergy (Elbersen, Fritsche, Overmars, et al., 2013; Elbersen, Fritsche, Petersen, et al., 2013; Frank et al., 2013; Nsanganwimana et al., 2014; Overmars et al., 2015; Plevin et al., 2014; Valin et al., 2015; Van der Laan et al., 2015) is that these are used for the production of biomass for biofuels instead of remaining unused. Expectations on the unused land availability, although difficult to make, indicate toward a large potential. Eitelberg et al. (2015) show a range in cropland availability at global level ranging from 1552 to 5131 Mha, including the 1550 Mha that is already cropland, so the additional part will need to come partly from lands regarded as abandoned.

A long-term analysis by Elbersen et al. (2020) for the EU only for the period between 1975 and 2016 of the utilized agricultural area (UAA) with Eurostat Farm Structural Survey (FSS) data showed a total decline for all EU-27 and United Kingdom of almost 36 million ha (18% of the UAA in 1975). Declines were seen over the whole period in all EU Member States, but the largest occurred in Bulgaria, Czechia, Estonia, Greece, Spain, Croatia, Italy, Cyprus, Latvia, Hungary, Poland, Slovenia, and Slovakia. In this same study by Elbersen et al. (2020), a land cover flow analysis was made showing that in 18 years (2000–2018), 8% of the agricultural land went out of agriculture.

Also, for the short-term future, agricultural land abandonment is expected to continue as was shown in Perpiña Castillo et al. (2021) for EU and United Kingdom. In total, the net agricultural land projected to flow into abandoned lands by 2030 amounts to 4.8 million ha. Another 600,000 ha is projected to flow into forest and natural areas and only 18,000 ha are projected to go to urban use by 2030. Spain is expected to lose even more than 1 million ha of agricultural land between 2015 and 2030. The study by Perpiña Castillo et al. (2021) also expects largest losses in the arable land taking up 70% of all abandonment in 2030 (around 4 million ha), while permanent grasslands and permanent crops make up 20% and 7%, respectively. In a separate study for Spain also by Perpiña Castillo et al. (2020), it is projected that until 2030, 5% of the total agricultural land will go out of use which is well above the 3% EU average.

The complex factors driving the process of abandonment have been discussed in several studies (e.g., Cvitanović et al., 2017; Elbersen et al., 2020; Filho et al., 2017; Keenleyside & Tucker, 2010; Lasanta et al., 2017; Pazúr et al., 2020; Perpiña Castillo et al., 2020; Pointereau et al., 2008; Terres et al., 2013, 2014) and show that the factors driving agricultural land abandonment can be categorized into four groups: natural constraints limiting the suitability for agricultural uses, socio-economic drivers at farm level, broader socio-economic drivers at regional level and drivers from policy (EU and national level). These factors can work out very differently depending on the local context (Perpiña Castillo et al., 2020). Alcantara et al. (2013) quantified the extent of abandoned farmland (cropland and pastures) in Central and Eastern Europe using satellite images. They found that abandoned farmland was widespread, totaling 52.5 million ha. The variation in rates of agricultural land abandonment across the area was driven to a large extent by differences in institutional and socio-economic factors among countries, rather than by biophysical settings. In Elbersen et al. (2020), in which drivers of agricultural land becoming abandoned were assessed through a literature review and through interviews in eight case studies spread over the EU, concluded that main drivers for agricultural land becoming abandoned are of socio-economic character, operating either at the level of the farm holding or of the region while natural constraints for agricultural land use and land degradation were not the most important drivers for agricultural land abandonment. Socio-economic drivers at farm level are the profitability of holdings, the productivity of the land for crops and livestock, production costs, fragmentation of farmland, and issues with land tenure and ownership. Depopulation of rural areas was the most frequently mentioned socio-economic driver at the regional level in Elbersen et al. (2020) together with factors as an

aging population, lack of transport infrastructure, and public services in rural areas.

Detecting when the land is really abandoned is challenging because it involves a gradual process of transition from agricultural land to shrubs and eventually forest. Goga et al. (2019) therefore proposes that when detecting with remote sensing (RS), the abandoned agricultural lands a uniform classification should be used for identifying the inner structure of progressive overgrowth change over time: Abandoned Agricultural Land (AAL1) overgrown by low vegetation (herbaceous formations); AAL2 overgrown by medium-sized vegetation (shrub formations) and AAL3 overgrown by tall vegetation (tree formations). How fast the different succession stages of vegetation are reached depends on local climate and soil conditions.

In Allen et al. (2014), the different stages of abandonment are discussed with a focus on underlying drivers. They reflect a complex process of reduced farming activity over a continuum, ranging from land that is temporarily unused (overlapping with short (1–2 year) or long (≥3 years) fallow) to semi-abandoned land (managed only to comply with CAP (Common Agricultural Policy) cross-compliance requirements but not currently used for production). At the end of the range is land that is entirely abandoned and where management is withdrawn completely. This is actual abandoned land where vegetation may change through natural succession into tall herb, bush, and forest ecosystems after a period, depending on climatic and soil conditions. On rich and wet soils, the outcome is likely to be forest ecosystems but, in contrast, on poor dry soils in Southeastern Europe, it can be "steppe-like" grassland vegetation that is able to survive for many years without any active management such as mowing or grazing. There is also a subcategory of abandoned land which Allen et al. (2014) called transitional abandonment. This category has been observed particularly in Central and Eastern Europe as a result of restructuring and land reforms but also other EU countries as a result of expected LUC or compulsory or voluntary set-aside (until abolished in 2008). Transitional abandonment can be seen also in areas that are economically marginal and they can move in and out of agricultural use depending on market prices applicable to the crops produced on them. It may also involve land that is held for optional conversion to urban or infrastructural use, but until that becomes official; the land may be kept into agricultural use to obtain CAP payments.

Land abandonment may have positive and negative impacts, which very much depend on local and wider regional context. Among the negative impacts, it can be mentioned that it may lead to a loss of valuable traditional landscapes and landscape management practices that help to support biodiversity, traditional cultural landscapes services, productive services (e.g., food and non-food products), provision of jobs and income, and prevent forest fires (e.g., Allen et al., 2014; Elbersen et al., 2020; Lasanta et al., 2017; Morell-Monzó et al., 2020; Perpina Castillo et al., 2018). Abandonment can also have positive effects if the successional vegetation that results leads to an additional build-up of above- and below-ground carbon and may lead to improved habitat quality, more landscape structural diversity, and habitats (rewilding) for certain wild species groups (Allen et al., 2014; Ceaușu et al., 2015; Morell-Monzó et al., 2020; Sačkov et al., 2020). Either way, the detection of where land abandonment takes place is relevant to be able to understand in an early stage the dynamics in land use and take measures to respond to the process in a timely way.

Several studies confirm that agricultural land abandonment in the EU is a large-scale phenomenon both in the past and in the near future which needs to be monitored and detected (Allen et al., 2014; Lasanta et al., 2017; Perpiña Castillo et al., 2020, 2021). Yet both in EU and national statistical sources, data on unused and abandoned land are not collected. The only unused land categories for which statistical data are collected refer to lands that are temporarily out of use, such as fallow land or temporarily unused lands. Also, if lands are unused for several years in a row, the lands lose their agricultural status and disappear from agricultural statistics (Elbersen et al., 2020). Wider land use statistics may still cover these lands, and register them according to the land use or land cover they have become. This can be forest, urban, nature conservation area, industrialized land, land used for recreation or transport, or a more undefined mixed class possibly more likely to be completely abandoned. However, the class "unused" or "abandoned" is nonexistent in both agricultural and wider land use statistics. The only source of information on abandoned lands in the EU is LUCAS (Land cover/use statistics, Eurostat). It identifies "fallow and abandoned land" as a separate land cover class, but since LUCAS only records this information in systematically selected points from a stratified area frame, the precise location and extend of these areas are not mapped.

1.1 | Identifying abandoned lands using RS

Several studies have mapped abandonment in agricultural lands through the use of RS data or a combination of different data and approaches, which have systematically been reviewed in Goga et al. (2019). Very different approaches are used. Most of the studies identify abandonment through changes in vegetation via indices

like Normalized Difference Vegetation Index (NDVI) EVI and TTVI calculations from time series (e.g., Alcantara et al., 2013; Estel et al., 2015; Han & Song, 2020; Kolecka, 2021; Terekhin, 2017). A study by Estel et al. (2015) used RS data (12 years-MODIS, 230 m) to detect farmland abandonment by calculating the Normalized Differenced Vegetation Index (NDVI) and determine the fallow frequency per grid in a 12-year period. The study found, for the area of Europe including also the whole of Turkey and the western half of Russia, that between 2001 and 2012, additional 7.6 million ha of land were abandoned. It was also found that there was widespread recultivation in this same period of up to 11.2 million ha and this occurred predominantly in Eastern Europe (e.g., European Russia, Poland, Belarus, Ukraine, and Lithuania) and in the Balkans. Estel et al. (2015) also described that detecting farmland abandonment through phenological changes using the NDVI index has limitations, which are cause by the coarse pixel size of MODIS images. They prevent the detection of land abandonment in smaller fields and highly heterogeneous landscapes.

There are also several studies that identify abandonment of agricultural land through the detection of land use or land cover changes in time (Campbell et al., 2008; Griffiths et al., 2013; Kuemmerle et al., 2011; Löw et al., 2015). Campbell et al. (2008), for example, analyses historic land use data detecting dynamics in land use and indirectly detects agricultural land abandonment. There are also several studies that use a more complex combination of satellite, in situ, and/or statistical data (e.g., Ceaușu et al., 2015; Milenov et al., 2014; Sackov, et al., 2020). An example is from Ceaușu et al. (2015) uses European specific data sources such as the potential net primary productivity and net harvested primary productivity, an index for travel time, potential natural vegetation, and night light impact. The last two indices were calculated from satellite data. More recent studies, for example, as implemented by Morell-Monzó et al. (2020, 2021) have used higher resolution satellite data from Sentinel-2 (10 and 20 m) and airborne imagery (1 m) for detecting land abandonment in a citrus production area in Valencia. The methodology involved a pixel-based classification applying the Random-Forest algorithm. The results showed that the use of the high-resolution information with the airborne images translated into Enhanced Vegetation Index (EVI) and Thiam's Transformed Vegetation Index (TTVI) delivered an accuracy of 88.5% correctly classified field plots. This was 77% in the case of using the 20 m Sentinel-2 images.

So far detection of abandonment is mostly performed by using optical RS-based indices such as NDVI, EVI, and TTVI. In more recent studies, the use of Synthetic Aperture Radar (SAR) information for the detection of land abandonment is seen. Yusoff et al. (2017) used it in combination with optical RS-data to distinct abandonment according to crop phenology in rubber, rice, and oil palm plantation areas in Malesia. The use of SAR data to detect grassland mowing/cutting events (and also the absence of these) was also applied in some studies (e.g., De Vroey et al., 2021; Taravat et al., 2019).

Given the observations from the former studies and the experiences of identification of abandoned lands, we have three main conclusions. Firstly, abandonment often involves a gradual process of transition from agricultural land to shrubs and eventually forest, it is difficult to detect with a uniform methodology taking vegetation indices only because the development of biomass varies very strongly in time with climate and soil. Furthermore, given differences in management systems, climate and soil classifications, it is difficult to determine exactly when land has become completely abandoned or whether it is still managed. Detecting abandonment based on land cover information or biomass development alone is therefore not sufficient. The management of the land, or actually the lack of it for several years in a row, needs to be detected by systematic data collection. Secondly, the detection of abandonment in smaller plots is a challenge. Therefore, for the detection higher resolution satellite data are recommended, particularly when areas are understudy with small-scale landscapes. Thirdly, most of the studies detecting abandonment use optical RS satellite-based indices and mostly focus on detecting changes in biomass development. A few studies have used SAR data.

Given the limitations and challenges in former studies, this study presents an alternative approach for identifying land abandonment using radar coherence data (in combination with a Random-Forest [RF] model). Radar data have several advantages compared to optical RS-data. Firstly, an inherent characteristic of land abandonment is the lack of land management (e.g., mowing, plowing, and harvesting), which implies that this needs to be detected. Radar coherence data are more informative in this respect because it enables to detect the stability (or lack of stability) in an object (explained further in Section 1.2). When fields are managed, they are “instable” because of plowing, sowing, harvesting, cutting/mowing activities. Capturing this instability, as a proxy for management, is not entirely captured through NDVI or other vegetation indices. Secondly, radar-based images are not influenced by cloud coverage, which is an advantage compared to optical RS-data which require time-intensive cloud masking first. Thirdly, the high spatial and temporal resolution of radar data provides the opportunity to identify abandoned lands for relatively large areas with a relatively small time investment once a methodology is working.

1.2 | Radar coherence—Detecting management activities

Interferometric coherence (further denoted as coherence) can be defined as the amplitude of the complex correlation coefficient between two complex SAR images (such as the Sentinel-1 SLC products) taken from different orbit positions and/or at different times. Coherence describes the similarity of the reflected radar signal between two images and varies between 0 (incoherent) and 1 (coherent). When the two images are taken of the same scene, with the same incident angle (same orbit) but at different times, the coherence provides information about the stability of the scattering surface (or target). Under such conditions, low coherence indicates that the surface has changed between the two observation dates, while high coherence indicates no changes, making coherence analysis particularly useful for detecting changes.

Many applications have been developed that use coherence techniques for change detection. These range from disaster monitoring in urban areas, land cover detection (Jacob et al., 2020), and crop monitoring. In the latter case, studies have shown that management activities such as mowing of grasslands (Abdel-Hamid et al., 2021; De Vroey et al., 2021; Taravat et al., 2019) and tilling, plowing, and harvesting activities (e.g., Shang et al., 2020) can be detected from coherence time series (whether or not in combination with other RS-data such as NDVI and backscatter information; Kavats et al., 2019; Khabbazan et al., 2019). The Sentinels for CAP—Sen4CAP project (http://esa-sen4cap.org/) has developed algorithms, products, and workflows and best practices, based among others on coherence data, for agriculture monitoring relevant for the management of the CAP.

In this study, it will be demonstrated that coherence data can be used to detect unused parcels in arable land in two provinces in Spain (Albacete and Soria). Section 2 presents the materials used and methods followed. It first gives an overview of data sources that have been used, and how these are prepared. This includes the processing of Sentinel-1 data and the preparation of parcel information. It then describes how coherence data (statistics) in combination with a RF model can be used to identify annual unused/used land maps and how these are combined to finally derive 4-year abandonment maps. In Section 4, the results of the proposed method are presented and validated followed by a discussion in the final section.

2 | MATERIALS AND METHODS

2.1 | Definition of abandoned land

For the development of a methodology to identify abandoned lands in this study, we follow the REDII definition of abandoned lands as discussed in the introduction. The focus is entirely on identifying abandonment in cropping land and not in permanent grassland. According to the definition in RED II, land is abandoned when it is not used for five consecutive years or more. In this study, we will first detect the absence of management on an annual basis, categorizing lands first as unused or used in case of detected management activities. When land is classified as unused for several consecutive years, it is considered abandoned.

2.2 | Study area

Our two study areas are the provinces of Albacete (14,926 km^2 and 11.7 inhabitants.km^2) and Soria (10,306 km^2 with 8.6 inhabitants.km^2), both situated in central Spain (Figure 1). Albacete has an average annual rainfall of 379 mm, is mostly located on the La Mancha plain (altitude of 686 m), and has a relatively cold and semiarid climate (Köppen: Bsk). Due to the continental climate regime, there is a large temperature variation throughout the year, the average temperature is 14.6°C. The soils in Albacete are dominantly calcareous (Calcisols and Calcic Luvisols, WRB 2015), weakly developed soils (Cambisols), and shallow and rocky soils (Leptosols). Land use is diverse with cereal production dominating in arable lands and large areas with perennial (permanent) crops such as vineyards, olives, and almonds. Olives and almonds grow more often in the steeper areas. In steeper

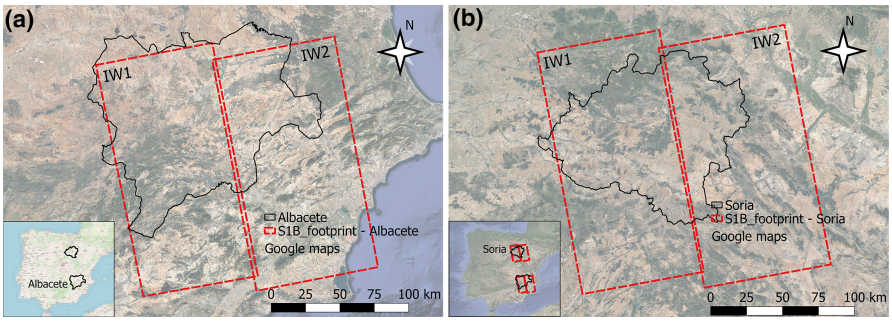

FIGURE 1 Map showing the study areas, provinces of Albacete (left panel—a) and Soria (right panel—b) in Central Spain, and the footprint of the used Sentinel-1B single-look complex data (sub-swath IW1 and IW2). Background: Google maps

areas with shallow soils, pine trees and permanent pasture are dominant.

Soria, at an altitude of 1000 m, has a temperate Atlantic climate (Köppen: Cfb). The average temperature in Soria is 10.7°C and annual rainfall is 511 mm. The soils are generally low in fertility with a dark topsoil (Umbrisols) in the western part, rich and weakly developed soils and shallow soils in the northern and eastern part, and calcaric soils in the southern part and alluvial soils in the river plains (Fluvisols). The main crops grown are wheat and barley and other grains cultivated are rye and triticale. A common rotation is sunflower–wheat–barley–sunflower.

In Soria, 2700–2800 kg grain per ha of wheat is produced on average. This average is lower for Albacete where it amounts to 1500 kg per ha in a normal year. The amount of marginal land share in both regions is high (Elbersen et al., 2018). Climate (cold and dry) is the dominant limiting factor followed by, locally, shallow and stony soils. Due to the relatively remote location of both provinces, income alternatives for small farmers, such as agro-tourism, is limited (Eupen et al., 2012).

During field visits in both areas and interviews performed with stakeholders in the regions (Elbersen et al., 2020), the five main factors mentioned and identified that drive land abandonment are: (1) depopulation and aging; (2) small parcels; (3) terrain quality—steep slopes, soil quality, and drought that makes it difficult to reach profit margins; (4) accessibility of the parcel (with machines); and (5) unresolved hereditary issues. Like in most regions in Spain, also Soria and Albacete have become confronted since 2010 with increasing cost levels for inputs (fertilizers, herbicides, seeds) in combination with low agricultural product prices and increasing impacts of climate change, notably lower rainfall and longer drought periods in several years (Ciria et al., 2019). This aspect will become a factor increasing land abandonment in the future (Ciria et al., 2019).

The application of rotational fallow in rainfed cereal-based production system is very common in the Mediterranean, including in the regions of Soria and Albacete where agricultural statistics (MAPA data) confirm that around 20% of the arable land is covered by fallow land. With the introduction of Greening through the CAP, the choice for rotational fallow as Ecological Focus Area (EFA) in this system was therefore by far the most frequently chosen (Díaz-Poblete et al., 2021). This aspect is important to keep in mind in our analysis because it implies that identifying unused lands that are unused for 1 year are very likely to be part of common rotational practices and/or allocated as EFA. For detection of abandonment, it is very important to get an understanding of longer term unused land status of at least three or more consecutive years.

2.3 | Sentinel-1 data

For the two study areas, all available single-look complex (SLC) images for the period 2017 up to 2020 of Sentinel-1B C-band SAR were collected (~30 SLC images per year, path 103 and ascending only); these images were processed into coherence images (resulting in ~29 coherence images per year). Images were taken from the Alaska Satellite Facility (https://asf.alaska.edu/). The interferometric-VV (Vertical-transmitting & Vertical-receiving) coherence (for subswatch IW1 and IW2, see Figure 2) was calculated from the 12-day Sentinel-1B image pairs using the ESA open-source software. In case of Albacete, the radar data cover roughly 90% of the province, and for Soria up to 95%.

Sentinel Applications Platform (SNAP, version 7.0) and Python 3.4 (and Python module snappy) were used for batch processing the RS-data. The VH-coherence was not used as it is less sensitive to changes occurring in the fields. This is also observed by Kavats et al. (2018, 2019) and Nasirzadehdizaji et al. (2021). One of the reasons for this is that VV is more sensitive to vegetation than VH due to vertical orientation of most vegetation. The processing steps for the derivation of coherence images were taken from Khabbazan et al. (2019). The spatial resolution of the final VV-coherence images was set at 20 × 20 m.

2.4 | SIGPAC data

For the selection of abandoned parcels in both Albacete and Soria, the data from the Geographical Information System of agricultural parcels (SIGPAC) of the Government of Spain (Ministry of Agriculture, Food and Environment)

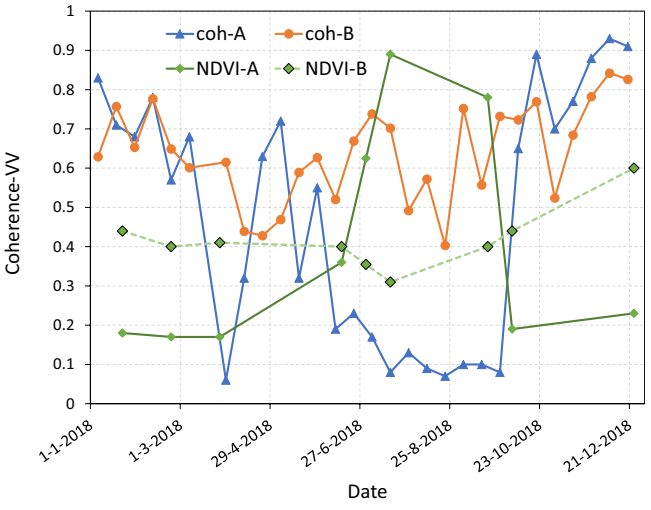

FIGURE 2 Annual time series of coherence and Normalized Difference Vegetation Index (NDVI) of a used arable land parcel (parcel A) and unused forested parcel (parcel B)

from 2018, 2019, and 2020 were used. SIGPAC provides information on land use (Table 1) and additional information on management with corresponding codes. Two of these codes are 117 "abandoned crop" (*cultivo abandonado*) and 158 "5-year-fallow" (*barbecho de 5 años*). Parcels that have these codes are considered abandoned.

In addition, the land use description of the parcels in SIGPAC was used to distinguish between arable land and permanent crops (other land use classes, e.g., grassland, were ignored). Parcels with mixed crops (e.g., olives + citrus, vineyards + olives) were excluded from the analysis. For the Albacete region, on average 6300 5-year-fallow parcels were found per year, equally divided between arable land (~3145) and permanent crops (~3177, of which half olive groves). The average parcel size of these 5-year fallow parcels was 0.7 ha.

The size of the selected fallow land SIGPAC parcels was reduced with a buffer of 20 m and finally rasterized into 20 × 20 m pixels. Shrinking of the parcels was done to have "pure" pixels and to avoid (field) border effects.

Table 2 gives an overview of the collected SIGPAC data for Albacete. The dataset covered in total 133,142 samples (i.e., 20 × 20 m pixels) within the land use class arable land, and consisted of 65,142 samples representing unused arable land and 68,000 randomly selected samples representing used arable land. The sample size of both groups (used vs. unused) was equally distributed and covers in total 5300 ha. The numbers between the brackets show the total number of fallow land samples when also permanent crops are added (which is ~15,000 samples extra).

TABLE 1 SIGPAC land use description and corresponding SIGPAC codes

SIGPAC land use description	SIGPAC codes
Arable land	TA
Permanent crops:	
Vineyards (wine or table grapes)	VI (vineyards), VF (table grapes)
Olive groves	OV (olives—oil), OF (table olives)
Fruit orchards	FY (mixed fruit)
Nut orchards	FS (nuts)
Citrus orchards	CI (citrus—mono-cult.), CS (citrus-mixed)
Permanent grassland	PS (grass), PR (grass with shrubs and trees), PA (grass with trees)
Forest	FO
Nonagricultural surfaces	AG (water), ED (urban built-up), EP, IM (unproductive), CA (roads), ZU (urban)
Other	ZV (censured)

2.5 | Proposed method

Management activities in arable land such as field preparations (plowing or tilling) but also harvesting are abrupt changes that take place in a field and have impact on radar coherence observations. Such events are mostly visible as spikes or sudden jumps in the coherence time series (Kavats et al., 2019; Voormansik et al., 2020). In case of harvesting, when the crop is completely removed from the field, the coherence tends to increase after such an event as scattering from the soil becomes dominant (Kavats et al., 2019). Crops typically show a low coherence (close to the noise floor, ~0.2) as crops are growing and move by the wind, which cause temporal decorrelation, and thus low coherence. Bare soils in general show a high coherence (similar to built-up areas) as these objects do not change (much) over time. Once a crop is removed completely from the field, bare soil becomes visible resulting in a jump in the coherence time series. Also plowing has an impact on the coherence. Voormansik et al. (2020)

TABLE 2 Number of samples (20 × 20 m pixels) representing unused and used arable land, that have been used for the training and validation of the Random-Forest-model for Albacete. The numbers between the brackets show the number samples when the permanent crop pixels are added[a]

Year	Unused cropping land pixels (SIGPAC)	Used cropping land pixels	Subtotal
2018	38,242 (40,207)	40,000 (40,000)	78,242 (80,207)
2019	13,320 (16,920)	14,000 (17,000)	27,320 (33,920)
2020	13,580 (16,916)	14,000 (17,000)	27,580 (33,916)
Total no. of 20 m pixels 2018–2020			133,142 (148,043)
For training (80%)			106,513 (118,434)
For validation (20%)			26,629 (29,609)

[a]The numbers between the brackets show the total number of samples when permanent crops are included (which is ~15,000 extra).

reported that plowing in general causes even larger jumps in the coherence signal.

Arable land that is being used and where management activities occur (i.e., plowing, tilling, and harvesting) will reveal a coherence time series that contains several (significant) spikes or jumps. Fields that are not used will not show such spikes or jumps. In case of unused bare fields, the mean coherence signal will be relatively high and stable with only small fluctuations. In case of unused (partly) vegetated fields, the coherence signal will likely show a lower mean coherence, but still quite stable and also with small fluctuations. Most of these fluctuations in the signal are caused by seasonal effects (e.g., rainfall, snow). This is demonstrated in Figure 2, which shows the annual coherence time series of two land parcels located in Albacete: an arable land parcel (parcel A) that is being used and a forested parcel that is not managed at all (parcel B). In addition, the NDVI time series are shown, which are based on Landsat 8 level-1T products (NDVI is calculated as the ratio between the red [R] and near-infrared [NIR] bands). The NDVI shows the development of the vegetation during the season. Clearly visible are the abrupt changes in coherence signal of parcel A and in spring and autumn. The sudden drop in coherence is caused by field preparations (plouwing and sowing) of the bare soil (NDVI <0.2). After this event, coherence slowly recovers to high values until the crop slowly emerges. In autumn, the crop is harvested (drop NDVI to 0.2), which results in sudden increase of the coherence. The forested parcel (parcel B) shows a more stable coherence (and NDVI) signal. The signal does show fluctuations, but these are smaller and are caused by weather (e.g., rainfall) and seasonal effects, which are also visible in the time series of the used parcel.

Instead of using an algorithm to determine the exact timing of management activities (as is done in most CAP-monitoring studies), it will be shown that the annual statistics of coherence time series can also be used to distinguish between unused and used parcels. This is shown in Figure 3 for a small area in Albacete. The upper left panel (Figure 3a) and right panel (Figure 3b) show the mean annual coherence and standard deviation of coherence based on 2018 coherence data. The lower panel (Figure 3c) shows the parcel boundaries and corresponding land use according to SIGPAC. The white parcels with black boundaries are arable land parcels that are being used. The white parcels with orange-colored boundaries are "5-year fallow" according to SIGPAC. The remaining (colored) parcels are permanent crops, forest and grassland parcels, urban areas, and other land cover classes. What strikes immediately is that the coherence statistics (mean and standard deviation) precisely follow the parcel boundaries. Forest, (extensive) grassland, and also urban areas show a low standard deviation (Figure 3b), as these areas are not managed intensively. This is also the case for the "5-year fallow" SIGPAC parcels. Many arable land parcels show a high(er) standard deviation, which suggests some level of management. However, the range in standard deviation between the fields is large. The spatial variation can also be seen in the annual mean coherence map (Figure 3a). In this figure, the mean coherence is colored between green (low coherence) and brown (high coherence). Since crops tend to have low coherence values and bare soil high values, the annual mean coherence can be seen as a (very simple) proxy for biomass. This can also be seen in Figure 2, where the coherence time series of parcel A behaves opposite to the NDVI time series (low coherence—high NDVI; high coherence—low NDVI).

The observed spatial variations in the standard deviation and mean coherence are caused by:

- Variations in crop type (arable vs. permanent crops, short and sparse vegetation vs. tall and dense vegetation) and the length of the growing season.
- Variations in the frequency and type of management activities, including irrigation practices, and their impact on coherence.

For example, rainfed-based cereal production systems (in Albacete) can be characterized as follows: field preparations of the bare soil in spring, followed by a short growing period (with no irrigation) and harvesting in autumn, where the crop is completely removed from the field (high impact on coherence; see parcel A in Figure 2). This will result in relatively high annual mean coherence (field is bare for a relative long period with a short crop season and no irrigation) and high standard deviation of coherence (both plowing and harvesting cause large fluctuations in the coherence signal). As the growing season expands, or irrigation is applied (more biomass in these arid conditions), the annual mean coherence will decrease and also affect the standard deviation.

Voormansik et al. (2020) reported that mowing activities in grassland in general cause (much) smaller jumps in the coherence signal than plowing. After plowing, the vegetation completely disappears, while in case of mowing, only part of the vegetation is removed. In case of permanent crops such as orchards (olives, fruit, and nuts) and also vineyards, it is expected that the impact of harvesting (and also other field management activities) on the coherence signal is also small, making it more difficult to distinguish between used and abandoned permanent crops (orchards, vineyards, and grasslands). The approach in this study will therefore only focus on detecting land abandonment in arable land where coherence in relation to arable land management or absence thereof is better understood.

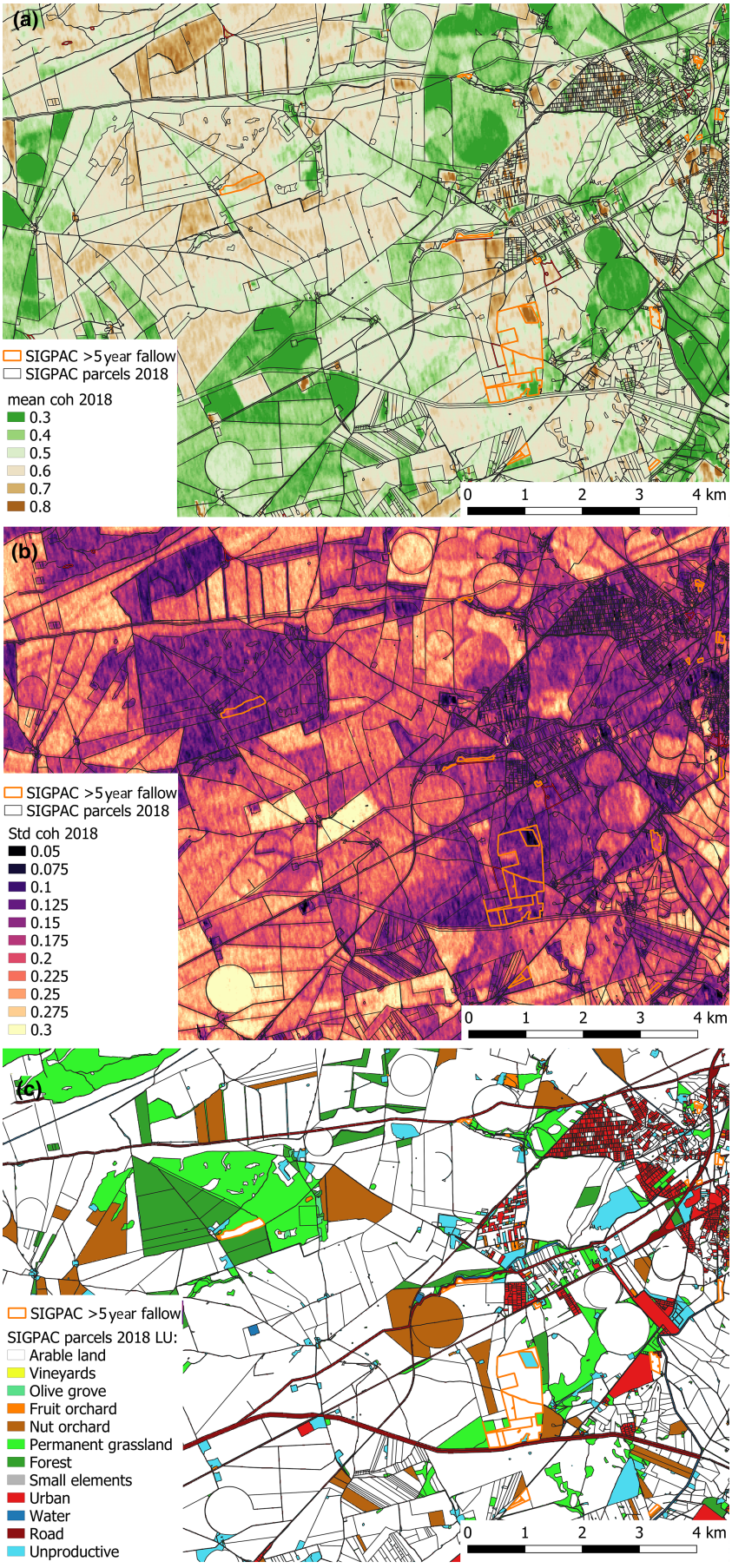

FIGURE 3 Subset Albacete. Upper left panel (a)—Annual mean coherence 2018, upper right panel (b)—Standard deviation of coherence 2018, lower panel (c)—Land use according to SIGPAC 2018

In order to distinguish between used and unused arable land based on the coherence statistics, the following dataset was prepared. For each year, a (pixel-based) statistical analysis based on the time series of VV-coherence images was conducted by deriving per quarter (representing the periods January–March; April–June; July–September; and October–December) the following six statistics:

- coherence (defined as coh):
  1: mean coh; 2: standard deviation of coh; 3: range coh
- change in coherence (defined as Dcoh = $\text{coherence}_{t1} - \text{coherence}_{t2}$):
  4: mean of Dcoh; 5: standard deviation of Dcoh; 6: maximum of Dcoh

This resulted in a set of six statistics per quarter, that is, 24 input variables (so-called predictors) in total per year. The reason it was decided to use quarterly statistics rather than annual is that we found slightly better results (training of a RF model). The standard deviation and range of coherence (*coh*) and the statistics of change in coherence (*Dcoh*) can be considered as indicators for the management intensity (used land: high values of standard deviation and range; unused land: low values of standard deviation and range). The mean coherence (*mean coh*) can be considered as an indicator of vegetation status (bare soil: high mean coherence vs. vegetated soils: low mean coherence) and can help to improve the distinction between used and unused land, due to variations in the coherence statistics caused by variations in crop type, length of growing season, and management activities (mentioned before).

The quarterly statistics, for the years 2017–2020 (maps of quarterly statistics at 20 × 20 m spatial resolution), will be combined with the collected SIGPAC data (Section 2.4) of used and unused cropping land pixels, to train a RF model.

A RF (or random decision forest) is a powerful but simple, data mining, and supervised machine learning technique. It allows quick and automatic identification of relevant information from extremely large datasets. One of the biggest advantages of RF is that it relies on the collection of many predictions (trees) rather than trusting one (Borcan, 2020). We have used the Scikit-learn free software machine learning library for Python (https://scikit-learn.org/stable/).

Figure 4 provides an overview (flowchart) of the entire approach adopted in this study. The first step involves the preparation of the time series of coherence maps (covering 4 years: 2017–2020, Section 2.3) and calculate from these the quarterly statistics of coherence (Section 2.4). Next, coherence statistics were combined with 3 years of SIGPAC land use data (containing fallow land parcels, covering the years 2018–2020, Section 2.4). From this combination, a training dataset was generated, which was used to train the RF-model (Section 3.1). The trained RF-model was then used to derive four annual maps of unused/used land for the period 2017–2020 (Section 3.1). Finally, these four annual maps were combined in a 4-year abandonment map, where land was classified as abandoned if not used for three consecutive years or more (Section 3.2).

3 | RESULTS

3.1 | Annual unused/used land maps arable land

3.1.1 | Albacete

For the training of the RF-model for Albacete, the number of trees of the model was set at 500 trees, and 80% of the collected SIGPAC parcel data was used (Table 2). The remaining 20% of the data was used for validation. Rather than training the RF-model for a single year, it was decided to train it for all 3 years combined (i.e., 2018, 2019, and 2020 together). This was done for two reasons. First, to create a larger dataset, as the number of training samples is limited per year (Table 2), and second, to avoid any seasonal effects between the years.

Table 3 shows the performance of the RF-model for Albacete, when the model is specifically trained for arable land. The validation is based on 20% of the dataset. The overall accuracy of the model is 88%, with a true-positive rate (TPR) of 0.87 and true-negative rate (TNR) of 0.89, meaning that the model can predict both classes of used (TPR) and unused (TNR) arable land well (87% of the used land and 89% of the unused land (according to SIGPAC) are correctly classified by the model).

The variable importance of the 11 most important predictors (i.e., the quarterly coherence statistics) is shown in Table 4. The table reveals which of the coherence statistics have the most predictive power. It was found that the mean coherence of the second quarter (period April–June) is by far the most important, followed by the standard deviation of coherence of the fourth quarter (period October–December). Then, there is a group of five predictors that roughly have the same importance. This group mainly consists of coherence statistics of the fourth quarter, except for the maximum change of coherence (*Dcoh*). The remaining (not shown) predictors have an importance of less than four.

Next, the trained RF-model was applied for each year (2017–2020) separately, in order to derive annual maps of unused/used land within the land use class arable land. A sample of the four annual unused/used land maps for 2017–2020 in Albacete is presented in Figure 5. The parcel boundaries (black polygons) and land cover classes are taken from SIGPAC, including SIGPAC parcels that are fallow for more

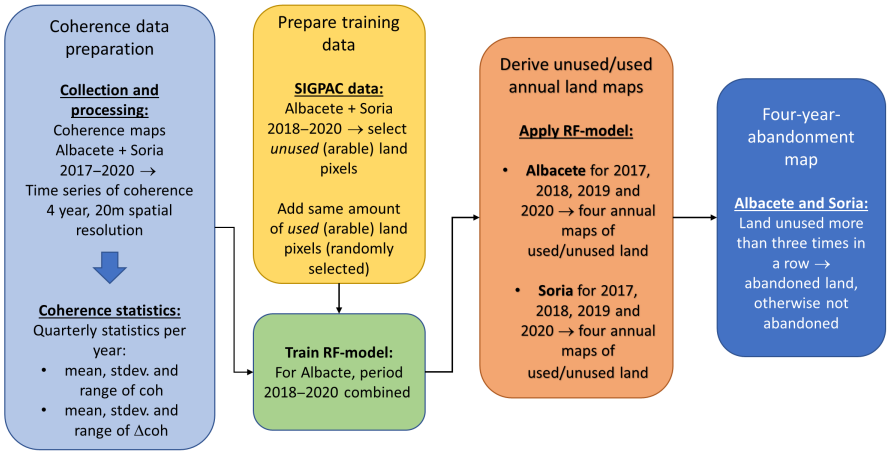

FIGURE 4 Flowchart of the methodology adopted in this study

TABLE 3 Confusion matrix for Albacete, Random-Forest (RF)-model trained for arable land only. Results are based on 20% subset of dataset (=26,629 samples)

	RF—Predicted			
	Used arable land	**Unused arable land**	**Total**	
Truth (SIGPAC 2018–2020)				
Used arable land	**11,819**	1753	13,572	**0.87** (TPR)
Unused arable land	1384	**11,673**	13,057	**0.89** (TNR)
Total	13,203	13,426	26,629	

than 5 years (orange polygons). The white parcels/areas in all four panels are used arable land parcels/areas according to both SIGPAC and the RF-based unused/used land maps. The colored areas (2017: light green, 2018: light yellow, 2019: light blue and 2020: light pink) are identified as unused arable land by the RF-model. Clearly visible is the annual rotation of unused arable land in the annual used/unused land maps. Furthermore, it can be seen that, in many cases, the unused land patterns of the RF-model follow the SIGPAC parcel boundaries very well, which demonstrates that the RF-model (based on the coherence statistics) is able to distinguish between parcels based on their management.

How good the results are for the whole province of Albacete is shown in Table 5. The model can predict unused land very well (TNR ranges between 0.96 and 0.98, i.e., 96%–98% is correctly classified as unused land). However, it underestimates the prediction of used land (TPR varies between 0.63 and 0.66, i.e., 63%–66% is correctly classified as used land). Overall it results in an accuracy that varies between 63% and 66%. Here, the model suggests that there is more unused land within the land use class arable land than SIGPAC reports. In fact, the model says that ~35% of the arable land in Albacete is not used in 2020. SIGPAC registers parcels that are fallow for 5 years or more. The main reason for this difference is the fact that on an annual basis, the model cannot distinct between parcels that are fallow for 1 year and parcels that are not used for multiple years (≥5 years). This is supported by the annual rotation of unused land in Figure 4, which demonstrates that parcels are sometimes not used. As mentioned in Section 2.2, the application of rotational fallow in rainfed cereal-based production system (used as EFA) is very common in the region of Albacete (and Soria), which is in the order of 20% of the arable land (according to the agricultural statistics (MAPA data)).

3.1.2 | Soria

To test the applicability of the RF-model to other areas, the RF-model trained for Albacete was applied to the province of Soria and compared with a locally trained RF-model (based on SIGPAC data of Soria). The collection of training data for Soria was identical to Albacete. The total number of training samples for Soria is 34,655 20 m pixels, consisting of 17,255 unused land pixels (taken from SIGPAC 2018 to 2020) and 17,400 randomly selected used land pixels (within land use class arable land). Similar to Albacete, samples for all 3 years were combined for training of the model (first, to have a larger training set, and second to avoid seasonal effects between the 3 years). Note that the dataset of Soria is a factor of four smaller than that of Albacete. The reason is that many SIGPAC fields in Soria are (on average) smaller, and in the end not usable for training once converted into 20 m pixels.

TABLE 4 Variable importance of the first 11 most important predictors. The numbers represent the first, second, third and fourth quarter of the year

	Variable	Importance
1	Mean coherence 2nd quarter	13.18
2	Std. deviation coherence 4th quarter	6.54
3	Mean coherence 3rd quarter	5.73
4	Std. deviation coherence 1st quarter	5.62
5	Maximum delta_coherence 4th quarter	5.28
6	Mean coherence 4th quarter	5.15
7	Range coherence 4th quarter	5.04
8	Mean delta_coherencecoherence 4th quarter	4.75
9	Std. deviation delta coherence 4th quarter	4.74
10	Range coherence 2nd quarter	4.07
11	Mean delta_coherence 3rd quarter	4.03

Table 6 shows the performance of the locally trained model for Soria. Also here the model is specifically trained for arable land using 80% of the collected SIGPAC data for Soria (period 2018–2020) and the remaining 20% was used for validation. The overall accuracy of the model was found to be 88%. The model is able to predict both classes of used (TPR) and unused (TNR) arable land well: 89% of the used land and 87% of the unused land (according to SIGPAC) are correctly classified by the model.

Next, both RF-models were applied to the years 2017–2020 separately for deriving the annual unused/used land maps for the whole province and validated with the SIGPAC data. These annual results are also presented in Table 6 (2018, 2019, and 2020). Note that the validation of these annual maps is based on the whole province. It was found that the locally trained RF-model predicts unused arable land better than the RF-model of Albacete: TNR of

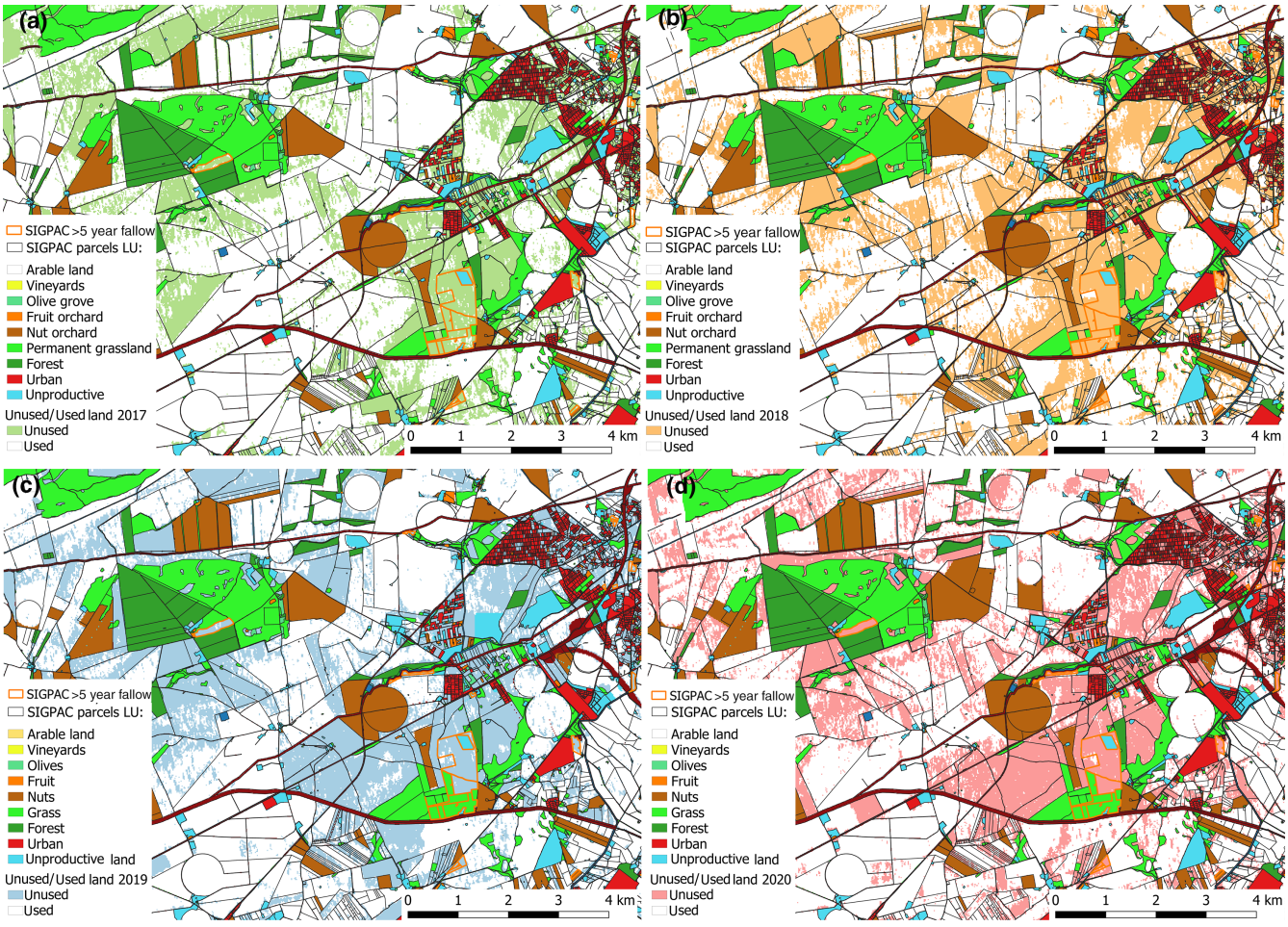

FIGURE 5 Samples of unused/used land maps in Albacete for 2017 (upper left (a)), 2018 (upper right (b)), 2019 (lower left (c)), and 2020 (lower right (d)). The parcel boundaries (black polygons) and land cover classes are taken from SIGPAC, including the SIGPAC parcels that are fallow for more than 5 years (orange polygons)

TABLE 5 Confusion matrix: unused/used land map for 2018, 2019, and 2020, based on the whole province of Albacete

	Random-Forest—Predicted			
Truth (SIGPAC)	**Used arable land**	**Unused arable land**	**Total**	
2018				
Used arable land	**7,655,365**	4,449,017	12,104,382	0.63 (TPR)
Unused arable land	883	**37,359**	38,242	0.98 (TNR)
Total	7,656,248	4,486,376	12,142,624	Accuracy: 63%
2019				
Used arable land	**7,864,867**	4,264,382	12,129,249	0.65 (TPR)
Unused arable land	254	**13,121**	13,375	0.98 (TNR)
Total	7,865,121	4,277,503	12,142,624	Accuracy: 65%
2020				
Used arable land	**7,952,332**	4,176,917	12,129,249	0.66 (TPR)
Unused arable land	474	**12,901**	13,375	0.96 (TNR)
Total	7,952,806	4,189,818	12,142,624	Accuracy: 66%

Bold used for calculating the TPR and the TNR.

TABLE 6 Overall accuracy of the locally trained Random-Forest (RF)-model for Soria, based on SIGPAC data from 2018 to 2020 combined. And the accuracy of the annual unused/used land maps for 2018, 2019, and 2020 for the whole province of Soria, based on the locally trained RF-model and based on the trained RF-model for Albacete

	RF-model (locally trained)			RF-model Albacete (applied to Soria)		
Truth (SIGPAC year)	**Accuracy**	**TPR (used land)**	**TNR (unused land)**	**Accuracy**	**TPR (used land)**	**TNR (unused land)**
2018–2020	88%[a]	0.89	0.87	×	×	×
2018	44%[b]	0.44	0.98	66%[b]	0.66	0.66
2019	44%[b]	0.44	0.90	68%[b]	0.68	0.68
2020	60%[b]	0.60	0.94	67%[b]	0.67	0.76

[a]Based on 20% of the SIGPAC dataset.

[b]Based on the whole province of Soria.

0.90–0.98 versus TNR of 0.66–0.76. However, for the classification of used arable land, the locally trained model is too sensitive (TPR varies between 0.44 and 0.6), that is, it classifies too many used land pixels as unused, resulting in a very low overall accuracy of 44% in 2018 and 2019 (and 60% in 2020). The RF-model trained for Albacete is worse in predicting unused land (TPR of ~0.67), but it is better in predicting used arable land (TNR of 0.66–0.76) in Soria. Overall, this leads to a slightly better accuracy of on average 67%.

The underestimation of used land (TPR between 0.66 and 0.76) by the RF-model trained for Albacete was also found for Albacete (Table 5). In both provinces, on an annual basis, roughly 66% of the used arable land (according to SIGPAC) is classified as used, while 34% is classified as unused. As explained before, this is the result of rotational fallow in rainfed-based cereal production system that are used as EFAs.

Figure 6 shows a sample of the annual unused/used land maps for Soria (for 2017–2020), based on the RF-model for Albacete (which performed slightly better than the locally trained model). The parcel boundaries, the land cover classes, and parcels that are fallow for more than 5 years (orange parcels) are taken from SIGPAC. The white parcels/areas in all four panels are used arable land/parcels according to both SIGPAC and the RF-based unused/used land maps. The colored areas (2017: light green, 2018: light yellow, 2019: light blue, and 2020: light pink) are identified as unused arable land by the RF-model. Similar to Albacete, the annual rotation of unused parcels is clearly visible, and in many cases, the unused patterns of the model follow the SIGPAC parcel boundaries very well.

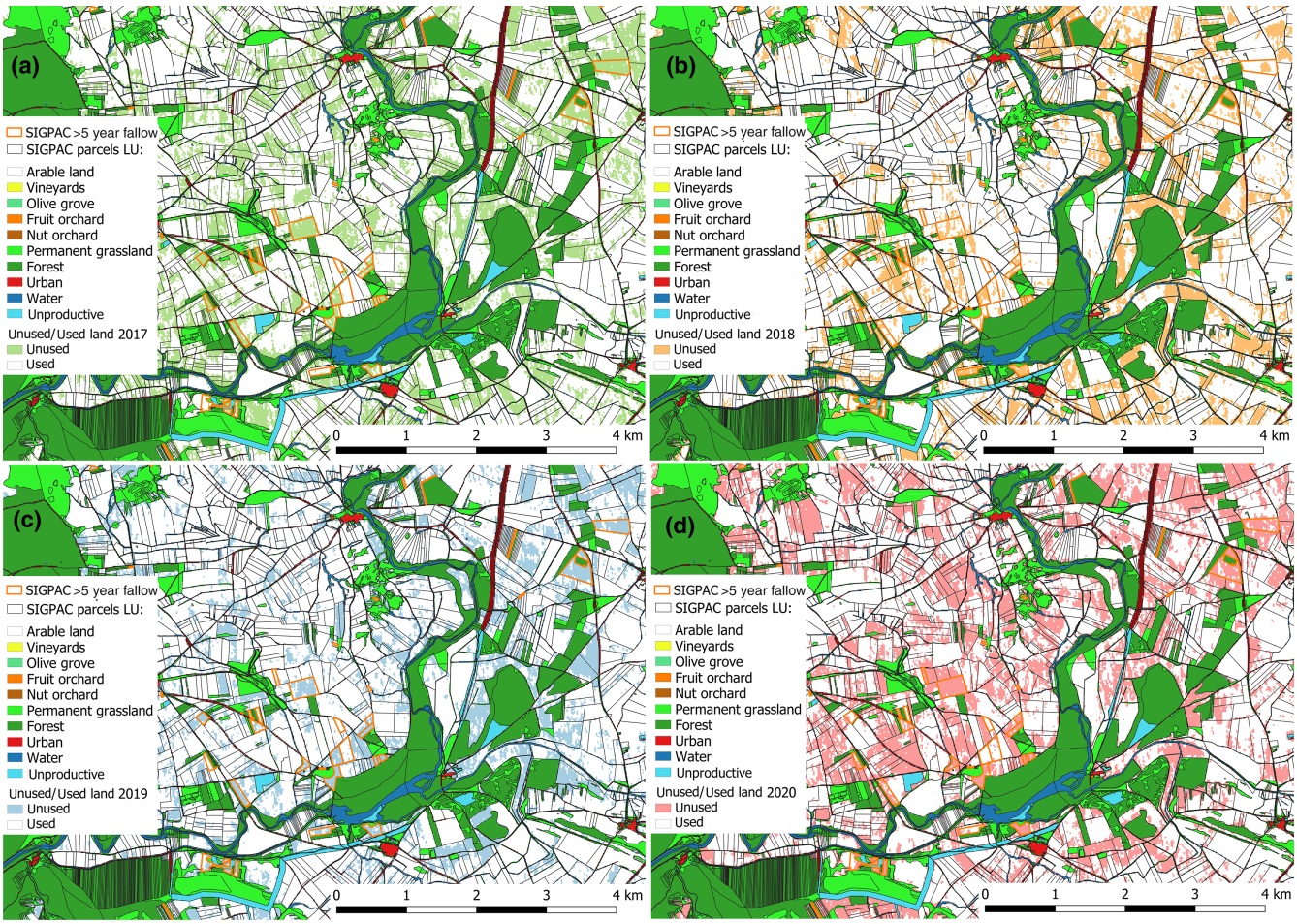

FIGURE 6 Samples of unused/used land maps in Soria for 2017 (upper left (a)), 2018 (upper right (b)), 2019 (lower left (c)), and 2020 (lower right (d)). The parcel boundaries (black polygons) and land cover classes are taken from SIGPAC, including the parcels that are fallow for more than 5 years (orange polygons)

TABLE 7 Confusion matrix: 4-year abandonment map (2017–2020) based on SIGPAC, for the whole province of Albacete

	Random-Forest—4-year abandonment map			
Truth	**Used arable land**	**≥3-year fallow arable land**	**Total**	
SIGPAC				
Used arable land	9,753,753	2,035,610	11,789,363	0.83 (TPR)
≥5 year fallow arable land	2004	11,576	13,580	0.85 (TNR)
Total	9,755,757	2,047,186	11,802,943	

3.2 | Four-year abandonment maps arable land

3.2.1 | Albacete

Based on the four annual unused/used land maps of 2017–2020, a 4-year abandonment map for Albacete was generated. When a 20-m pixel is not used for 3 years or more in a row, it is considered as abandoned; otherwise, it is classified as used arable land. Table 7 shows a detailed confusion matrix based on SIGPAC ≥5 year fallow data and for the whole province of Albacete. The overall accuracy is 83%. Of the 13,580 SIGPAC pixels within the class arable land that have been unused for 5 years (or more) over the period 2017–2020, 11,576 pixels are also unused according to the RF-based 4-year abandonment map (a TNR of 0.85). Of the 11,789,363 pixels that are used arable land according to SIGPAC, 83% is also used land according to the 4-year abandonment map (a TPR of 0.83).

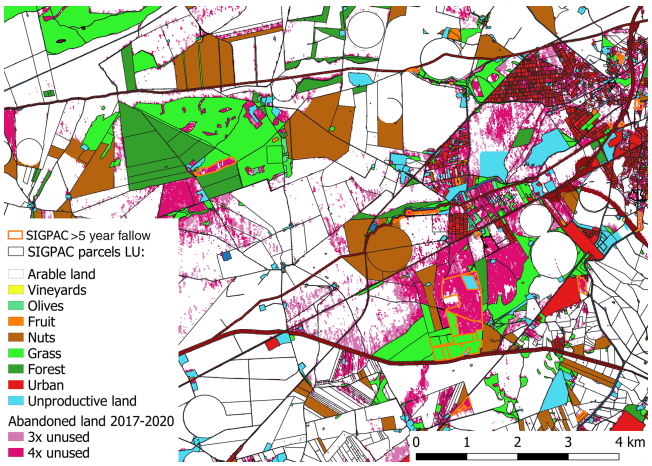

FIGURE 7 Sample of the 4-year abandonment map in Albacete (period 2017–2020). The parcel boundaries (black polygons) and land cover classes are taken from SIGPAC. The orange-colored parcels are registered in SIGPAC as ≥5-year fallow. The white parcels/areas are used arable land according to both SIGPAC and the 4-year abandonment map. The pink-colored areas (light and dark) are identified as unused in the 4-year abandonment map

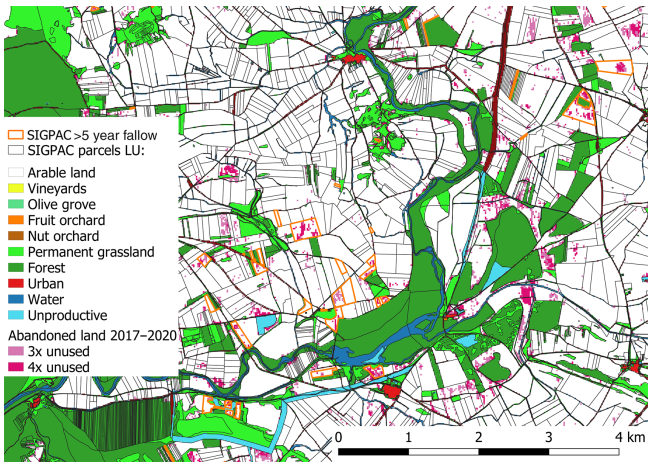

FIGURE 8 Sample of the 4-year abandonment map in Soria (period 2017–2020). The parcel boundaries (black polygons) and land cover classes are taken from SIGPAC. The orange-colored parcels are registered in SIGPAC as ≥5-year fallow. The white parcels/areas are used arable land according to both SIGPAC and the 4-year abandonment map. The pink-colored areas (light and dark) are identified as unused in the 4-year abandonment map

A sample of the 4-year abandonment map for Albacete is presented in Figure 7. Parcel boundaries, land cover classes, and parcels that are fallow ≥5 years are taken from SIGPAC. All permanent crops and land cover classes other than arable land are colored. The remaining white parcels/areas are used arable land according to SIGPAC. Pixels that are classified as used arable land in the 4-year abandonment map are also white, and pixels that are unused for ≥3 years are light pink or dark pink. It can been seen that most of the SIGPAC ≥5-year fallow parcels (orange colored) are also identified as unused in the 4-year abandonment map. The 4-year abandonment map shows some scattered pixels; however, most of unused land pixels are concentrated in a small set of parcels.

3.2.2 | Soria

Similar to Albacete, the 4-year abandonment map for the province of Soria was derived. It is based on the four annual unused/used land maps determined with the RF-model that was trained for Albacete. The confusion matrix, showing the accuracy of the 4-year abandonment map, is shown in Table 8. It is also based on SIGPAC data and shows the situation for the whole province of Soria. Although the overall accuracy is 88.5%, the model is less able to classify unused arable land correctly: a TNR of 0.48, that is, roughly 50% of the unused land (according to SIGPAC) is classified as unused in the 4-year abandonment map.

A sample of the 4-year abandonment map for Soria is shown in Figure 8. Parcel boundaries and land use information are taken from SIGPAC (including parcels that are registered as ≥5 year fallow, labeled as orange). White parcels/areas are used arable land according to both SIGPAC and the 4-year abandonment map. The pink-colored pixels/areas are classified as abandoned in the 4-year abandonment map. The underestimation of unused land in the RF-based 4-year abandonment map (a low TNR of 0.48 in Table 8) is also visible in the figure as most of the ≥5-year fallow SIGPAC parcels (orange) are not classified properly as unused in the 4-year abandonment map. In many cases, a small fraction of the parcels are pink colored.

4 | DISCUSSION

In this study, it is demonstrated that (quarterly) statistics of radar coherence data can be used for detecting abandonment in arable land when these statistics are used to train a RF model. Firstly, the annual maps of unused/used arable land for the years 2017–2020 clearly show annual "rotational fallow" land and the unused/used patterns follow the SIGPAC parcel boundaries. This demonstrates that the coherence statistics (and RF-model) in general can distinguish between parcels based on their management. Secondly, the trained RF-model using the statistical indices derived from radar coherence data was successful in predicting unused/used arable land.

For the annual unused/used land maps for the whole province of Albacete, the model prediction has an accuracy

TABLE 8 Confusion matrix: 4-year abandonment map (2017–2020) based on SIGPAC, for the whole province of Soria

	Random-Forest—4-year abandonment map			
Truth	**Used arable land**	**≥3-year fallow arable land**	**Total**	
SIGPAC				
Used arable land	7,740,577	1,005,700	8,746,277	0.89 (TPR)
≥5-year fallow arable land	1232	1118	2350	0.48 (TNR)
Total	7,741,809	1,006,818	8,748,627	

of roughly 66%. Although the model is able to predict unused arable land very well (97% of the SIGPAC fallow land is classified as unused), the prediction of used arable land is underestimated (only 65% of the used arable SIGPAC land is classified as used, see Table 6). This implies that the model suggests that there is more unused land within the land use class arable land than SIGPAC reports. The reason that the RF-model detects more unused arable land on an annual basis is likely caused by rotational fallow of rainfed cereal production land, which is used as EFA, a common practice in Mediterranean areas such as Albacete (and Soria). SIGPAC includes only parcels that are fallow for 5 years or longer (and does not include EFA-practices). The RF-model cannot distinguish between land that is fallow for 1 year and land that is fallow for a number of years.

Applying the trained RF-model on the whole territory of Albacete for all 4 years (2017–2020) resulted in a 4-year abandonment map with an overall accurate prediction of 83%. As the effect of EFA practices is now filtered out, the model is able to predict both classes of used and abandoned arable land well (a TPR of 0.83 and TNR of 0.85, see Table 7).

To determine whether the trained model was also effective in predicting unused/used arable land in other regions, the model was also applied to Soria. It was found that the RF-model trained in Albacete performed slightly better than the locally trained RF-model of Soria. The most logical reason for this is the limited number of training samples available for Soria, as compared to Albacete (34,655 samples for Soria vs. 133,142 samples for Albacete). The limited number of 20 m samples in Soria is the result of two factors: (1) less fallow land parcels in Soria and (2) on average smaller land parcels in Soria (average parcel size of 0.4 ha vs. 0.6 ha in Albacete). As the polygons of these parcels are reduced in size before being converted to 20 m pixels, less pixels remain. Although the RF-model of Albacete works better than the locally trained model, the results for Soria are not as good as was found for Albacete. Other factors that may explain lower predictive power in Soria are likely to be related to differences in climate that lead to differences in timing of crop development and application of management practices. Soria region is located more centrally and at overall higher altitude then the region of Albacete and therefore has a colder climate and a shorter growing season and slightly higher precipitation levels.

To further investigate the applicability in other regions, the RF-model trained for Albacete was also applied in the Italian region of Emilia-Romagna (Northern Italy). Even though both regions are characterized by a Mediterranean climate, the precipitation levels are very different. In Emilia-Romagna, the average annual precipitation more than doubles that of Albacete (and that of Soria). For Emilia-Romagna region, LPIS (Land Parcel Identification Systems) data were available for the years 2018, 2019, and 2020. Similarly, to SIGPAC (Spain), LPIS data contain information at parcel level, including a code (COD_COLT) and description (DESC_COLT) of land use and management. Using the RF-model in Emilia-Romagna showed initially that the model strongly underestimated the classification of unused parcels in Emilia-Romagna. Only 25% of the fallow-LPIS-parcels were classified as unused. When the RF-model was locally trained based on LPIS data (3 years), the model was able to classify unused land much better; however, the model became too sensitive (such as was experienced in Soria), resulting in an overestimation of the fraction of unused land (almost 50% of the land was classified as unused). Possible reasons why the predictive power of both the externally trained and locally trained RF-models is not so satisfactory for Emilia-Romagna are:

1. The large difference in average annual precipitation. In Emilia-Romagna, the evolution of vegetation in unused lands is much faster and rapidly tends toward shrub development.
2. Because of climatic differences, the tuning of land and crop management operations are likely to be differently timed between both regions.
3. Unused parcels in Emilia-Romagna are small, and as a result, the number of training samples (20 m pixels) was relatively small in the locally trained RF-model (as was the case in Soria). The smaller the training samples the lower the predictive quality of the RF-model becomes.

4. In the LPIS for Emilia-Romagna, long-term abandonment for more than 5 years is not registered, as is the case in SIGPAC (for Spanish regions), but only fallow at an annual basis. But also the LPIS-codes for fallow land are difficult to interpret correctly for Emilia-Romagna as these may as well cover rotational fallow practices, which in practice only involve the absence of management for a couple of months per year and not for an entire year. Furthermore, among the several types of fallow land codes, there are also categories for fallow with a nature conservation objective. For these fallow parcels, farmers are still expected to cut vegetation, even though this has not a productive purpose and it is done to either avoid obtaining a fine or to avoid losing the long-term agricultural status (and therefore the CAP payment right). The radar coherence signals in these cases are not the same as for complete cessation of management. Overall, it can therefore be concluded that it is difficult to determine to what extend inaccurate predictions of unused/used arable land is caused by the low RF-model quality or by the unclear and incomplete registration of fallow practices in LPIS. After all, an RF-model can only be trained effectively on accurate data.

Finally, the RF-model was also trained in a combination of arable and permanent cropping land (which included vineyards, olive groves, and fruit, nut, and citrus orchards). From this assessment done for Albacete (for detailed results, see Supporting Information I), it became clear that the detection of abandonment in permanent crops was not as accurate as it was for arable land. We therefore conclude that the trained RF-model for Albacete is only acceptably accurate for predicting unused/used lands in arable cropping land and not in permanent cropping land. The first reason for this low accuracy in permanent cropping land was related again to the relatively small training dataset available in permanent cropping land (the total dataset contains only 10% permanent crops). Secondly, crop management activities/or absence of those in arable land are much more distinctive and uniform then in permanent cropping land, which consisted of a diverse suit of crops and related practices. Thirdly, the (type of) management activities in arable lands are much more destructive for soil and vegetation and generally translate in high standard deviation in coherence signals than management practices in, for example, orchards, which are generally less frequent and drastic. Because of this, the training of the RF-model for a combination of arable and permanent croplands in Albacete resulted in a predictive model that is too sensitive. It overestimated unused land in permanent crops (in particularly orchards).

There are still several limitations connected to our combined method using radar coherence data and a RF model to detect unused cropping lands. The first limitation is that a good model can only be developed if there are sufficient training samples. The second limitation is that the detection of land abandonment in regions with very steep slopes is likely to be more difficult because radar signals are less reliable in such areas. This is explained by the fact that when using coherence techniques for detecting changes at the ground, it is important that the signals recorded at a given location in the two SAR images are correlated while in steed slopes, this may not be the case. The coherence consists of a spatial component and a temporal component. Here, we are interested in the temporal component, which reflects changes in the physical properties of the target (or object), caused by land management activities (or the lack of). Changes in the target will affect the temporal component of coherence. Therefore, it is important that the spatial component does affect the coherence too. The spatial component is dependent on the geometric properties of the satellite acquiring the images and the ground surface. Decorrelation of the spatial component can be caused by small changes in the satellite viewing geometry between the acquisitions and can be stronger in areas of steep topography as it is dependent on incidence angle (Borrows at al., 2020; Jacob et al., 2020). It is therefore likely that the coherence data in mountainous areas are less accurate (reliable) for detecting unused cropping land than in flat areas.

The third limitation is that our method is limited to a minimum field size. Although the coherence data have a high spatial resolution (20 m) and can cover relatively small fields, edge effects are to be avoided, which implies that very small and also narrow fields/areas cannot be monitored accurately. This is a limitation particularly because we know from literature (Alcantara et al., 2013; Lasanta et al., 2017; Terres et al., 2014) that small fields are abandoned sooner than large fields. In case of Soria, many fields were excluded from the training set because of their small field size and avoidance of edge effects.

The fourth limitation is that the presented method shows promising results for detection of abandonment in arable lands, but not for permanent crops. Beside the fact that this was caused in this study by the small number of training samples, the more important challenge is that management activities in most permanent crops (except for vineyards) are not easily detectable via coherence data. The method implemented by Morell-Monzó et al. (2020, 2021) to detect abandonment of permanent crops (mostly citrus) in the region of Valencia is considered relevant and likely to be an alternative but only where it involves local studies. Morell-Monzó et al. (2020, 2021) used higher resolution satellite data and also airborne imagery (1 m) for

detecting land abandonment also in combination with a RF model. The results showed that the use of the high-resolution information with the airborne images translated into EVI and TTVI delivered an accuracy of 88.5% correctly classified field plots. However, the limitation of Morell-Menzo et al.'s approach is that it will be very difficult and time consuming to obtain and process (e.g., the cloud screening) all high-resolution data and therefore very difficult to apply and roll-out the approach to larger regions in Europe. The application will only need to serve a local need rather than a national or EU wide need for information on the location and scale of abandonment.

The fifth limitation is the Sentinel-1 archive. In this study, Sentinel-1B data of 2017–2020 were used. This could be expanded to 6 years by adding Sentinel-1A, which is available for 2015–2016. Six-year data are still limited given the need for training datasets that cover a longer period for the detection of longer term abandonment. It does suffice currently for identifying the low ILUC lands defined in the EU Recast RED II, which need to be unused for at least 5 years. Over the next years, more SAR data will become available, making the application of the methodology easier and more accurate.

Finally, there is also a need for obtaining good training data from national and regional LPIS data in different regions of the EU, which contain reliable data on unused land status of agricultural parcels. So far, the information from the Spanish LPIS (SIGPAC) proved useful, but this was not the case for the LPIS data from Emilia-Romagna. In general, it is not easy to access LPIS data, even more for the additional attribute information layers on management of land or absence of it. Every paying agency in the EU countries and regions handles data access differently. A more central coordination on how to access the LPIS data will help getting a better understanding of the abandonment situation in Europe and will facilitate the improvement of our method to detect land abandonment in a much larger area and in a wider number of climatic zones in Europe.

Overall, we conclude that the results in this paper showed the potential of the presented method using radar coherence data and a RF model to detect abandonment in arable lands. The results demonstrated clearly that the coherence statistics (and RF-model) in general can distinguish between parcels based on their management. The trained RF-model was successful in predicting 4-year abandonment in arable land in Albacete with an overall accuracy of 83%.

The developed RF-model did not prove effective so far in predicting land abandonment in permanent crops (such as vineyards and fruit/nut/citrus orchards and olive groves). Further efforts need to be invested, also building on relevant work done by Morell-Monzó et al. (2020, 2021), to make the abandonment detection in these types of crops widely possible.

To improve the applicability of the radar coherence data and RF model approach to a wider number of EU regions, there are still several limitations that need to be addressed. Firstly, there is an urgent need for making available high-spatial and temporal resolution radar data over the next years. Secondly, improving quality of and access to LPIS data would be very helpful to create training datasets for developing and improving our methodology further to detect land abandonment in a much larger and climatically diverse areas of Europe.

The need to develop the early detection of abandonment is important. It can help to take the necessary measures to reverse this process of abandonment, to detect no-go areas and areas with opportunities to create win–win situations between production of low-ILUC biomass for the bioeconomy and environmentally and socio-economically sustainable land use practices. It will also indicate where action needs to be taken to ensure that land abandonment does not lead to unwanted adverse effects on environment, biodiversity, ecosystem services, and rural livelihoods. Whether these adverse effects occur is determined by the local context.

The approach presented here, which is based on radar coherence data, is more promising than when it is based on NDVI or NVI indices from optical satellite imagery. In our opinion, radar information has many advantages in detecting land abandonment. Land abandonment is the lack of land management activities, which implies that radar coherence data, unlike NDVI or NVI, are currently the only more informative source of data that enables to detect the stability (or lack of stability) caused by land management in a field. Furthermore, radar-based images provide a more complete multispatial and time-series information because they are not influenced by cloud coverage and therefore provides a database, which is more complete and less time consuming to prepare then with optical satellite data (e.g., Sentinel-2 and Landsat), or other high-resolution airborne imagery. Finally, the high spatial and temporal resolution of radar images provides the opportunity to identify abandoned lands for relatively large areas with a relatively small time investment once a methodology is working with a high detection accuracy.

ACKNOWLEDGMENTS

This research received funding from the European Union's Horizon 2020 Research and Innovation Program under grant agreement No 727698. We also thank the University of Hohenheim for supporting the publication of this

paper in this special issue. Finally, we thank the Spanish Ministry of Agriculture, Fisheries and Food (MAPA) for making available the information from SIGPAC.

CONFLICT OF INTEREST

The authors declare no conflict of interest.

DATA AVAILABILITY STATEMENT

All data that support the findings of this study are available in the paper or in Supporting Information of this article.

ORCID

Berien Elbersen https://orcid.org/0000-0001-8709-9004
Andrea Parenti https://orcid.org/0000-0003-0551-1232
Andrea Monti https://orcid.org/0000-0003-3480-726X

REFERENCES

Abdel-Hamid, A., Dubovyk, O., & Greve, K. (2021). The potential of sentinel-1 InSAR coherence for grasslands monitoring in Eastern Cape, South Africa. *International Journal of Applied Earth Observation and Geoinformation*, *98*, 102306. https://doi.org/10.1016/j.jag.2021.102306

Alcantara, C., Kuemmerle, T., Baumann, M., Bragina, E., Griffiths, P., Hostert, P., Knorn, J., Muller, D., Prishchepov, A., Schierhorn, F., Sieber, A., & Radeloff, V. (2013). Mapping the extend of abandoned farmland in Central and Eastern Europe using MODIS time series satellite data. *Environmental Research Letters*, *8*(3), 035035.

Allen, B., Kretschmer, B., Baldock, D., Menadue, H., Nanni, S., & Tucker, G. (2014). *Space for energy crops—Assessing the potential contribution to Europe's energy future*. Report produced for BirdLife Europe, European Environmental Bureau and Transport and Environment London; IEEP.

Borcan. (2020). https://programmerbackpack.com/introduction-to-random-forests-classifier-and-step-by-step-sklearn-implementation/(visited30-9-2021)

Borrows, K., Walters, R. J., Milledge, D., & Densmore, A. (2020). A systematic exploration of satellite radar coherence methods for rapid landslide detection. *Natural Hazards and Earth System Sciences*, *20*(11), 3197–3214. https://doi.org/10.5194/nhess-20-3197-2020

Campbell, J. E., Lobell, D. B., Genova, R. C., & Field, C. B. (2008). The global potential of bioenergy on abandoned agriculture lands. *Environmental Science & Technology*, *42*(15), 5791–5794.

Ceaușu, S., Hofmann, M., Navarro, L., Carver, S., Verburg, P., & Pereira, H. (2015). Mapping opportunities and challenges for rewilding in Europe. *Conservation Biology*, *29*(4), 1017–1027.

Ciria, C. S., Sanz, M., Carrasco, J., & Ciria, P. (1833). Identification of arable marginal lands under rainfed conditions for bioenergy purposes in Spain. *Sustainability*, *11*(7), 1833. https://doi.org/10.3390/su11071833

Cvitanović, M., Lučev, I., Fürst-Bjeliš, B., Borčić, L. S., Horvat, S., & Valožić, L. (2017). Analyzing post-socialist grassland conversion in a traditional agricultural landscape—Case study Croatia. *Journal of Rural Studies*, *51*, 53–63. https://doi.org/10.1016/j.jrurstud.2017.01.008

Daioglou, V., Woltjer, G., Elbersen, B., Barberena Ibanez, G., Strengers, B., Sanches Gonzales, D., & van Vuuren, D. (2020). Progress and barriers in understanding and preventing indirect land use change. *Biofuels, Bioproducts and Biorefining*, *14*(5), 924–934.

De Vroey, M., Radoux, J., & Defourny, P. (2021). Grassland mowing detection using Sentinel-1 time series: Potential and limitations. *Remote Sensing*, *13*, 348. https://doi.org/10.3390/rs1303034

Díaz-Poblete, C., García-Cortijo, M. C., & Castillo-Valero, J. S. (2021). Is the greening instrument a valid precedent for the new green architecture of the CAP? The case of Spain. *Sustainability*, *13*, 5705. https://doi.org/10.3390/su13105705

EC Directorate-General for Research and Innovation. (2018). A sustainable Bioeconomy for Europe: strengthening the connection between economy, society and the environment. Updated bioeconomy strategy. In *EU Recast Renewable Energy Directive (RED II)*. EC. https://doi.org/10.2777/478385

Edwards, R., Mulligan, D., & Marelli, L. (2010). *European Commission—Joint Research Centre indirect land use change from increased biofuels demand*. https://www.energy.eu/publications/Indirect-Land-Use-Change-from-increased-Biofuels-Demand.pdf

Eitelberg, D., van Vliet, J., & Verburg, P. (2015). A review of global potentially available cropland estimates and their consequences for model-based assessments. *Global Change Biology*, *21*, 1236–1248. https://doi.org/10.1111/gcb.12733

Elbersen, B. S., Fritsche, U., Overmars, K., Lesschen, J. P., Staritsky, I., Ros, J., Zulka, K. P., Brodski, L., Eerens, H., & Hennenberg, K. (2013). *Review of the EU bioenergy potential from a resource efficiency perspective. Background report to EEA study*. A follow-up to EEA report No 7/2006. ETC-SIA technical report. ETCSIA.

Elbersen, B. S., Fritsche, U. R., Petersen, J.-E., Lesschen, J. P., Böttcher, H., & Overmars, K. (2013). Assessing the effect of stricter sustainability criteria on EU biomass crop potential. *Biofuels, Bioproducts and Biorefining*, *7*, 173–192. https://doi.org/10.1002/bbb.1396

Elbersen, B., Hart, K., Koper, M., van Eupen, M., Keenleyside, C., Verzandvoort, S., Kort, K., Cormont, A., Giadrossi, A., & Baldock, D. (2020). *Analysis of actual land availability in the EU trends in unused, abandoned and degraded (non) agricultural land and use for energy and other non-food crops*. Reference: ENER/C2/2018-440

Elbersen, B. S., van Eupen, M., Boogaard, H. L., Mantel, S., Verzandvoort, S. J. E., Mücher, C. A., Ceccarelli, T., Elbersen, H. W., Bai, Z., Iqbal, Y., Cossel, M., MCallum, I., Carrasco, J., Ramos, C., Monti, C. D., Scordia, D., & Eleftheriadis, I. (2018). *Deliverable 2.6 Methodological approaches to identify and map marginal land suitable for industrial crops in Europe*. https://doi.org/10.5281/zenodo.3539311

Estel, S., Kuemmerle, T., Alcántara, C., Levers, C., Prishchepov, A., & Hostert, P. (2015). Mapping farmland abandonment and recultivation across Europe using MODIS NDVI time series. *Remote Sensing of Environment*, *163*, 312–325. https://doi.org/10.1016/j.rse.2015.03.028

ETC/SIA. (2013). *Review of the EU bioenergy potential from a resource efficiency perspective. Background report to EEA study*. Alterra.

Eupen, M., Metzger, M. J., Perez-Soba, M., Verburg, P., van Doorn, A., & Bunce, R. G. H. (2012). A rural typology for strategic European policies. *Land Use Policy*, *29*, 473–482.

Fargione, J. E., Plevin, R. J., & Hill, J. D. (2010). The ecological impact of biofuels. *Annual Review of Ecology, Evolution, and Systematics*, *41*, 351–377.

Filho, W. L., Mandel, M., Quasem, A., Feher, A., & Chiappetta Jabbour, C. (2017). An assessment of the causes and consequences of agricultural land abandonment in Europe. *International Journal of Sustainable Development & World Ecology*, *24*(6), 554–560. https://doi.org/10.1080/13504509.2016.1240113

Frank, S., Böttcher, H., Havlík, P., Valin, H., Mosnier, A., Obersteiner, M., Schmid, E., & Elbersen, B. (2013). How effective are the sustainability criteria accompanying the European Union 2020 biofuel targets? *GCB Bioenergy*, *5*(3), 306–314. https://doi.org/10.1111/j.1757-1707.2012.01188.x

Goga, T., Feranec, J., Bucha, T., Rusnák, M., Sačkov, I., Barka, I., Kopecká, M., Papčo, J., Oťaheľ, J., Szatmári, D., Pazúr, R., Sedliak, M., Pajtík, J., & Vladovič, J. (2019). A review of the application of remote sensing data for abandoned agricultural land identification with focus on central and Eastern Europe. *Remote Sensing*, *11*, 2759. https://doi.org/10.3390/rs11232759

Griffiths, P., Müller, D., Kuemmerle, T., & Hostert, P. (2013). Agricultural land change in the Carpathian ecoregion after the breakdown of socialism and expansion of the European Union. *Environmental Research Letters*, *8*, 045024.

Han, Z., & Song, W. (2020). Abandoned cropland: Patterns and determinants within the Guangxi Karst Mountainous Area, China. *Applied Geography*, *122*, 102245. https://doi.org/10.1016/j.apgeog.2020.102245

Jacob, A. W., Vicente-Guijalba, F., Lopez-Martinez, C., Lopez-Sanchez, J. M., Litzinger, M., Kristen, H., Mestre-Quereda, A., Ziółkowski, D., Lavalle, M., Notarnicola, C., & Suresh, G. (2020). Sentinel-1 InSAR coherence for land cover mapping: A comparison of multiple feature-based classifiers. *IEEE Journal of Selected Topics in Applied Earth Observations and Remote Sensing*, *13*, 535–552. https://doi.org/10.1109/JSTARS.2019.2958847

Kavats, A., Khramov, D., Sergieieva, K., Vasyliev, V., & Kavats, Y. (2018). Geoinformation technology of agricultural monitoring using multi-temporal satellite imagery. In *Proceedings of the ICAG 2018: 20th International Conference on Agriculture And Geoinformatics*, Menlo Park, CA, 14–15 June 2018.

Kavats, O., Khramov, D., Sergieieva, K., & Vasyliev, V. (2019). Monitoring harvesting by time series of Sentinel-1 SAR data. *Remote Sensing*, *11*(21), 2496.

Keenleyside, C., & Tucker, G. M. (2010). *Farmland abandonment in the EU: An Assessment of trends and prospects*. Report prepared for WWF. Institute for European Environmental Policy.

Khabbazan, S., Vermunt, P., Steele-Dunne, S., Ratering Arntz, L., Marinetti, C., van der Valk, D., & Van der Sande, C. (2019). Crop monitoring using Sentinel-1 data: A case study from the Netherlands. *Remote Sensing*, *11*(16), 1887.

Kolecka, N. (2021). Greening trends and their relationship with agricultural land abandonment across Poland. *Remote Sensing of Environment*, *257*, 112340.

Kuemmerle, T., Olofsson, P., Chaskovskyy, O., Baumann, M., Ostapowicz, K., Woodcock, C. E., Houghton, R. A., Hostert, P., Keeton, W. S., & Radeloff, V. C. (2011). Post-Soviet farmland abandonment, forest recovery, and carbon sequestration in western Ukraine. *Global Change Biology*, *17*, 1335–1349.

Lasanta, T., Arnáez, J., Pascual, N., Ruiz-Flaño, P., Errea, M. P., & Lana-Renault, N. (2017). Space–time process and drivers of land abandonment in Europe. *Catena*, *149*(3), 810–823. https://doi.org/10.1016/j.catena.2016.02.024

Löw, F., Fliemann, E., Abdullaev, I., Conrad, C., & Lamers, J. P. A. (2015). Mapping abandoned agricultural land in Kyzyl-Orda, Kazakhstan using satellite remote sensing. *Applied Geography*, *62*, 377–390.

Milenov, P., Vassilev, V., Vassileva, A., Radkov, R., Samoungi, V., Dimitrov, Z., & Vichev, N. (2014). Monitoring of the risk of farmland abandonment as an efficient tool to assess the environmental and socio-economic impact of the Common Agriculture Policy. *International Journal of Applied Earth Observation and Geoinformation*, *32*, 218–227.

Morell-Monzó, S., Estornell, J., & Sebastia-Frasquet, M. T. (2020). Comparison of Sentinel-2 and high-resolution imagery for mapping land abandonment in fragmented areas. *Remote Sensing*, *12*(12), 2062.

Morell-Monzó, S., Sebastiá-Frasquet, M. T., & Estornell, J. (2021). Land use classification of VHR images for mapping small-sized abandoned citrus plots by using spectral and textural information. *Remote Sensing*, *13*(4), 681.

Nasirzadehdizaji, R., Cakir, Z., Sanli, F. B., Abdikan, S., Pepe, A., & Calò, F. (2021). Sentinel-1 interferometric coherence and backscattering analysis for crop monitoring. *Computers and Electronics in Agriculture*, *185*, 106118.

Nsanganwimana, F., Pourrut, B., Mench, M., & Douay, F. (2014). Suitability of Miscanthus species for managing inorganic and organic contaminated land and restoring ecosystem services. A review. *Journal of Environmental Management*, *143*, 123–134. http://www.sciencedirect.com/science/article/pii/S0301479714002163

OECD. (2018). *Effective carbon rates 2018: Pricing carbon emissions through taxes and emissions trading*. OECD Publishing. https://doi.org/10.1787/9789264305304-en

Overmars, K., Edwards, R., Padella, M., Prins, A. G., & Marelli, L. (2015). *Estimates of indirect land use change from biofuels based on historical data*. Joint Research Centre—Institute for Energy and Transport.

Pazúr, R., Lieskovský, J., Bürgi, M., Müller, D., Lieskovský, T., Zhang, Z., & Prishchepov, A. V. (2020). Abandonment and recultivation of agricultural lands in Slovakia—Patterns and determinants from the past to the future. *Land*, *9*, 316. https://doi.org/10.3390/land9090316

Pelkmans, L., Van Dael, M., Panoutsou, C., & Alakangas, E. (2016). *D6.3 Policy options to mobilize sustainable non-food biomass resources for the biobased economy*. S2BIOM Project Grant Agreement n°608622.

Perpiña Castillo, C., Coll Aliaga, E., Lavalle, C., & Martínez Llario, J. C. (2020). An assessment and spatial modelling of agricultural land abandonment in Spain (2015–2030). *Sustainability*, *12*(2), 560.

Perpiña Castillo, C. P., Jacobs-Crisioni, C., Diogo, V., & Lavalle, C. (2021). Modelling agricultural land abandonment in a fine spatial resolution multi-level land-use model: An application for the EU. *Environmental Modelling & Software*, *136*, 104946.

Perpina Castillo, C., Kavalov, B., Diogo, V., Jacobs-Crisioni, C., Batista e Silva, F., & Lavalle, C. (2018). *Agricultural land abandonment in the EU within 2015-2030 (No. JRC113718)*. Joint Research Centre (Seville site). www.ec.europa.eu/jrc/en/publications%0Ahttps://ec.europa.eu/jrc/en/publication/eur-scientific-and-technical-research-reports/agricultural-land-abandonment-eu-within-2015-2030%0Ahttps://ec.europa.eu/jrc/sites/jrcsh/files/jrc113718.pdf

Plevin, R. J., Beckman, J., Golub, A. A., Witcover, J., & O'Hare, M. (2015). Carbon accounting and economic model uncertainty of emissions from biofuels-induced land use change. *Environmental Science & Technology*, *49*(5), 2656–2664.

Plevin, R. J., Delucchi, M. A., & Creutzig, F. J. (2014). Using attributional life cycle assessment to estimate climate-change mitigation benefits misleads policy makers. *Journal of Industrial Ecology*, *18*, 73–83.

Pointereau, P., Coulon, F., Girard, P., Lambotte, M., Stuczynski, T., Sánchez Ortega, V., & Del Rio, A. (2008). *Analysis of farmland abandonment and the extent and location of agricultural areas that are actually abandoned or are in risk to be Abandoned*. EUR 23411EN. Institute for Environment and Sustainability, JRC.

Sačkov, I., Barka, I., & Bucha, T. (2020). Mapping aboveground woody biomass on abandoned agricultural land based on airborne laser scanning data. *Remote Sensing*, *12*(24), 4189. https://doi.org/10.3390/rs12244189

Searchinger, T., Heimlich, R., Houghton, R. A., Dong, F., Elobeid, A., Fabiosa, J., Tokgoz, S., Hayes, D., & Yu, T. H. (2008). Use of US croplands for biofuels increases greenhouse gases through emissions from land-use change. *Science*, *319*(5867), 1238–1240.

Shang, J., Liu, J., Poncos, V., Geng, X., Qian, B., Chen, Q., Dong, T., Macdonald, D., Martin, T., Kovacs, J., & Walters, D. (2020). Detection of crop seeding and harvest through analysis of time-series Sentinel-1 interferometric SAR data. *Remote Sensing*, *12*, 1551. https://doi.org/10.3390/rs12101551

Taravat, A., Wagner, M., & Oppelt, N. (2019). Automatic grassland cutting status detection in the context of spatiotemporal Sentinel-1 imagery analysis and artificial neural networks. *Remote Sensing*, *11*(6), 711. https://doi.org/10.3390/rs11060711

Terekhin, E. A. (2017). Recognition of abandoned agricultural lands using seasonal NDVI values. *Computer Optics*, *41*, 719–725.

Terres, J. M., Hagyo, A., Wania, A., Confalonieri, R., Jones, B. V., Diepen, K., & Van Orshoven, J. (2014). *Scientific contribution on combining biophysical criteria underpinning the delineation of agricultural areas affected by specific constraints. Methodology and factsheets for plausible criteria combinations*. JRC92686. https://doi.org/10.2788/844501

Terres, J. M., Nisini, L., & Anguiano, E. (2013). *Assessing the risk of farmland abandonment in the EU*. Publications Office of the European Union, European Union.

Thrän, D., Seidenberger, T., Zeddies, J., & Offermann, R. (2010). Global biomass potentials—Resources, drivers and scenario results. *Energy for Sustainable Development*, *14*(3), 200–205.

Valin, H., Peters, D., Van den Berg, M., Frank, S., Havlik, P., Forsell, N., Hamelinck, C., Pirker, J., Mosnier, A., Balkovic, J., & Schmidt, E. (2015). *The land use change impact of biofuels consumed in the EU: Quantification of area and greenhouse gas impacts*. ECOFYS.

Van der Laan, C., Wicke, B., & Faaij, A. P. C. (2015). *Strategies to mitigate indirect land use change: Illustrated for palm oil production in North and East Kalimantan*. Copernicus Institute of Sustainable Development, Utrecht University.

Voormansik, K., Zalite, K., Sünter, I., Tamm, T., Koppel, K., Verro, T., Brauns, A., Jakovels, D., & Praks, J. (2020). Separability of mowing and ploughing events on short temporal baseline Sentinel-1 coherence time series. *Remote Sensing*, *12*(22), 3784.

World Reference Base (WRB) for Soil Resources 2014. (2015). *World soil resources reports 106*. FAO.

Yusoff, N. M., Muharam, F. M., Takeuchi, W., Darmawan, S., & Abd Razak, M. H. (2017). Phenology and classification of abandoned agricultural land based on ALOS-1 and 2 PALSAR multitemporal measurements. *International Journal of Digital Earth*, *10*, 155–174.

SUPPORTING INFORMATION

Additional supporting information may be found in the online version of the article at the publisher's website.

How to cite this article: Meijninger, W., Elbersen, B., van Eupen, M., Mantel, S., Ciria, P., Parenti, A., Sanz Gallego, M., Perez Ortiz, P., Acciai, M., & Monti, A. (2022). Identification of early abandonment in cropland through radar-based coherence data and application of a Random-Forest model. *GCB Bioenergy*, *14*, 735–755. https://doi.org/10.1111/gcbb.12939